J|A|C|S
ARTICLES
Published on Web 07/03/2004

Mechanism for Catechol Ring-Cleavage by Non-Heme Iron Extradiol Dioxygenases

Per E. M. Siegbahn* and Fredrik Haeffner

Contribution from the Department of Physics, Stockholm Centre for Physics, Astronomy and Biotechnology (SCFAB), Stockholm University, S-106 91 Stockholm, Sweden

Received February 4, 2004; E-mail: ps@physto.se

Abstract: The catalytic mechanism of the non-heme iron extradiol dioxygenases has been studied using hybrid density functional theory. These enzymes cleave a C−C bond outside the two hydroxyl groups of catechols, in contrast to the intradiol enzymes which cleave the C−C bond between these two groups. The chemical models used comprise about 70 atoms and include the first-shell ligands, two histidines, one glutamate, and one water, as well as some second-shell ligands, two histidines, one aspartate, and one tyrosine. Catechol is found to bind as a monoanion in agreement with experiments, while dioxygen is found to replace the water ligand. A spin-transition from the initial septet to a quintet state prepares the system for formation of a bridging peroxide with the catechol substrate. When the O−O bond is cleaved in the suggested rate-limiting step, a key substrate intermediate with partly radical and partly anionic character is formed. The partly anionic character is found to determine the selectivity of the enzyme. The results are compared to available experimental information and to previous studies.

I. Introduction

The extradiol dioxygenases are non-heme Fe(II)-containing enzymes that cleave the C−C bond adjacent to the hydroxyl groups of catecholic substrates, producing 2-hydroxymuconaldehyde acids. They belong to the general class of dioxygenases which are characterized by activating dioxygen and incorporating both oxygen atoms into their substrates.[1−3] In contrast to the extradiol dioxygenases, the intradiol dioxygenases use Fe(III) to degrade catechol to *cis*,*cis*-muconic acid with cleavage of the C−C bond between the two hydroxyl groups of catechol (see Figure 1). Both of these groups of enzymes play important environmental roles by facilitating microbial aerobic degradation of catechol and substituted catechol substrates,[4] and they have received much attention since they were first discovered by Hayaishi[5] and Dagley and Stopher[6] in the 1950s.

High-resolution X-ray structures of both intra- and extradiol dioxygenases, with and without bound catechol substrates, have been determined.[7−12] The active site of the 2,3-dihydroxybiphenyl 1,2-dioxygenase (BphC) from *Burkholderia* strain LB400 with the catechol substrate is shown in Figure 2. The coordination around the ferrous center is octahedral, with two histidines, His210 and His146, a glutamate, Glu260, and one water molecule. The catechol fills the two remaining coordination sites. A tyrosine residue, Tyr250, in the second coordination sphere hydrogen bonds to the catechol and to a histidine, His241. Other nearby residues are His195, which hydrogen bonds to the water ligand, and Asp244. Concerning the water ligand, it should be noted that the occupation of this position is only partial.[12] In two recent studies, this position has even been suggested to be empty[13,14] so that Fe(II) is five-coordinate rather than six-coordinate after the catechol substrate has been bound.

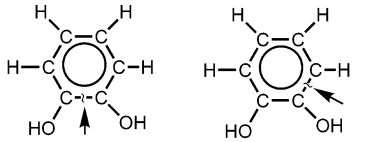

Figure 1. The different ways intra- and extradiol dioxygenases cleave catechols.

In addition to the BphC enzyme, the 2,3-CTD, the 4,5-CTD, and human homogentisate extradiol dioygenase enzymes (classes II and III) have been characterized and their structures determined with X-ray crystallography.[15,16] The 2,3-CTD and 4,5-

(1) Que, L., Jr.; Ho, R. Y. N. *Chem. Rev.* **1996**, *96*, 2607−2624.
(2) Solomon, E. I.; Brunold, T. C.; Davis, M. I.; Kemsley, J. N.; Lee, S.-K.; Lehnert, N.; Neese, F.; Skulan, A. J.; Yang, Y.-S.; Zhou, J. *Chem. Rev.* **2000**, *100*, 235−249.
(3) Bugg, T. D. H. *Tetrahedron* **2003**, *59*, 7075−7101.
(4) Bugg, T. D. H.; Winfield, C. *J. Nat. Prod. Rep.* **1998**, *15*, 513−530.
(5) Hayaishi, O.; Katagiri, M.; Rothberg, S. *J. Am. Chem. Soc.* **1955**, *77*, 5450.
(6) Dagley, S.; Stopher, D. A. *Biochem. J.* **1959**, *73*, 16P.
(7) Han, S.; Eltis, L. D.; Timmis, K. N.; Muchmore, S. W.; Bolin, J. T. *Science* **1995**, *270*, 976−980.
(8) Senda, T.; Sugiyama, S.; Narita, H.; Yamamoto, T.; Kimbara, K.; Fukuda, M.; Sato, M.;Yano, K.; Mitsui, Y. *J. Mol. Biol.* **1996**, *255*, 735.
(9) Ohlendorf, D. H.; Lipscomb, J. D.; Weber, P. C. *Nature* **1988**, *336*, 403.
(10) Orville, A. M.; Elango, N.; Lipscomb, J. D.; Ohlendorf, D. H. *Biochemistry* **1997**, *36*, 10039.
(11) Orville, A. M.; Lipscomb, J. D.; Ohlendorf, D. H. *Biochemistry* **1997**, *36*, 10052.
(12) Vaillancourt, F. H.; Han, S.; Fortin, P. D.; Bolin, J. T.; Eltis, L. D. *J. Biol. Chem.* **1998**, *273*, 34887.
(13) Sato, N.; Uragami, Y.; Nishizaki, T.; Takahashi, Y.; Sazaki, G.; Sugimoto, K.; Nonaka, T.; Masai, E.; Fukuda, M.; Senda, T. *J. Mol. Biol.* **2002**, *321*, 621−636.
(14) Davis, M. I.; Wasinger, E. C.; Decker, A.; Pau, M. Y. M.; Vaillancourt, F. H.; Bolin, J. T.; Eltis, L. D.; Hedman, B.; Hodgson, K. O.; Solomon, E. I. *J. Am. Chem. Soc.* **2003**, *125*, 11214−11227.
(15) Sugimoto, K.; Senda, T.; Aoshima, H.; Masai, E.; Fukuda, M.; Mitsui, Y. *Structure* **1999**, *7*, 953.

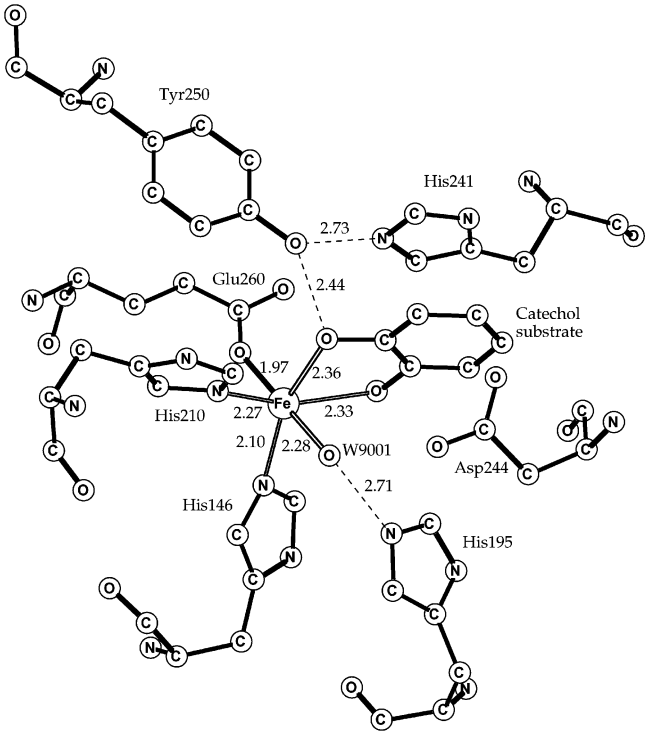

Figure 2. X-ray structure of the region around the non-heme iron center in 2,3-dihydroxybiphenyl 1,2-dioxygenase from strain LB400 complexed with catechol.[12] Distances are given in angstroms.

CTD enzymes, found in *Pseudomonas putida mt-2* and *Sphingomonas paucimobilis*, and human homogentisate dioygenase share no sequence similarity, nor do they have a similar structural fold. Still, their active sites are very similar, with two histidines and one glutamate coordinating the Fe(II) cofactor.

A range of molecules have been demonstrated to be substrates, but also inhibitors are known for these enzymes. Eltis and co-workers studied the inhibitory effects of 3-methylcatechol, 3-ethylcatechol, and catechol on the activity of 2,3-dihydroxybiphenyl 1,2-dioxygenase. They speculated that the inhibitory effect is due to the inability of the smaller substrates (compared to the larger 2,3-dihydroxybiphenyl) to fill the active site and hence protect the iron center from exposure to oxidation and inactivation (oxidative inactivation of the enzyme). 2,3-Dihydroxybiphenyl has a higher turnover rate than catechol (higher k_{cat}) and also a higher binding affinity (lower K_M).[31]

A large amount of spectroscopic data is available for the extradiol dioxygenases.[1,2,7,8,17−28] Experiments suggest that the extradiol dioxygenases catalyze the oxidation of their substrates via a so-called ordered mechanism, where the substrate coordinates to the Fe(II) center before oxygen binds.[20,23,29] Another question that has been studied is that of the number of protons available to take part in the ring-fission reaction, which is most likely of central importance. Considering that the pK_a value of catechol is around 9, and that these enzymes operate at physiological pH, it seems reasonable that the catechol substrate enters the active site neutral of charge. Upon chelation to Fe(II), it gives up one or two protons to nearby bases. On the basis of Raman spectroscopy and structural evidence, it has been proposed that catechol binds as a monoanion to Fe(II) in the extradiol dioxygenases.[12,18,30] Recently, Eltis and co-workers provided firm evidence, by using UV resonance Raman spectroscopy and electronic absorption spectroscopy, that 2,3-dihydroxybiphenyl is indeed monoanionic when bound to the Fe(II) ion in the extradiol 2,3-dihydroxybiphenyl 1,2-dioxygenase.[31]

Just as knowledge of the protonation state of the catechol when bound to Fe(II) is vital for understanding the detailed molecular mechanism, so is knowledge of the coordination and activation of O_2. There is no X-ray structure of any dioxygen-bound complex for any extradiol dioxygenase, but there is a structure of a BphC−substrate−NO complex, where the NO molecule occupies the equatorial position trans to Glu260, replacing the water ligand in Figure 2.[13] This position is in line with earlier suggestions based on studies using NO inhibitors.[31,32] On the other hand, Deeth and Bugg argue in a recent density functional study that O_2 may bind to Fe(II) in an axial position.[33]

The most accepted mechanism for how O_2 is activated is one where an electron is passed from the chelated catechol monoanion via Fe(II) to O_2, forming a semiquinone and a superoxide radical anion.[18,27] Bugg et al. have provided indications for the presence of radicals using spin-trap experiments in which they used a modified catechol comprising a cyclopropyl spin-trap substituent.[34]

His195, Tyr250, His241, and Glu260 have been suggested to act as bases: they deprotonate catechol when it binds to Fe(II), and later on they protonate the superoxide radical anion (with the same proton). Depending on how O_2 binds (equatorially or axially), His195, Tyr250, or Glu260 could act as a proton-mediator. It is, in principle, possible that one of the waters bound to iron before the catechol substrate binds in reality is a hydroxide and could therefore act as a base. However, the Fe−O distances are 2.4 and 2.1 Å for LB400 DHBD and 2.5 and 2.1 Å for KKS102 DHBD,[32] which do not indicate hydroxide ligands. Furthermore, it is the water with the longest Fe−O distance that appears to be lost when catechol binds. Therefore, the present study does not consider the possibility that a hydroxide ligand should act as a base.

(16) Titus, G. P.; Mueller, H. A.; Burgner, J.; Rodriguez de Cordoba, S.; Penalva, M. A.; Timm, D. E. *Nat. Struct. Biol.* **2000**, *7*, 542.
(17) Arciero, D. M.; Lipscomb, J. D.; Huynh, B. H.; Kent, T. A.; Münck, E. *J. Biol. Chem.* **1983**, *258*, 14981−14991.
(18) Shu, L.; Chiou, Y.-M.; Orville, A. M.; Miller, M. A.; Lipscomb, J. D.; Que, L., Jr. *Biochemistry* **1995**, *34*, 6649−6659.
(19) Harpel, M. R.; Lipscomb, J. D. *J. Biol. Chem.* **1990**, *265*, 22187−22196.
(20) Arciero, D. M.; Orville, A. M.; Lipscomb, J. D. *J. Biol. Chem.* **1985**, *260*, 14035−14044.
(21) Sato, M.; Yano, K.; Mitsui, Y. *J. Mol. Biol.* **1996**, *255*, 735−752.
(22) Bertini, I.; Capozzi, F.; Dikiy, A.; Happe, B.; Luchinat, C.; Timmis, K. N. *Biochem. Biophys. Res. Commun.* **1995**, *215*, 855−860.
(23) Mabrouk, P. A.; Orville, A. M.; Lipscomb, J. D. *J. Am. Chem. Soc.* **1991**, *113*, 4053−4061.
(24) Bertini, I.; Briganti, F.; Mangani, S.; Nolting, H. F.; Scozzafava, A. *Biochemistry* **1994**, *33*, 10777−10784.
(25) Chiou, Y. M.; Que, L., Jr. *Inorg. Chem.* **1995**, *34*, 3577−3578.
(26) Bertini, I.; Briganti, F.; Mangani, S.; Nolting, H. F.; Scozzafava, A. *FEBS Lett.* **1994**, *350*, 207−212.
(27) Arciero, D. M.; Lipscomb, J. D. *J. Biol. Chem.* **1986**, *261*, 2170−2178.
(28) Lin, G.; Reid, G.; Bugg, T. D. H. *J. Am. Chem. Soc.* **2001**, *123*, 5030−5039.
(29) Hori, K.; Hashimoto, T.; Nozaki, M. J. *Biochemistry* **1973**, *12*, 375−384.
(30) Uragami, Y.; Senda, T.; Sugimoto, K.; Sato, N.; Nagarajan, V.; Masai, E.; Fukuda, M.; Mitsui, Y. *J. Inorg. Biochem.* **2001**, *83*, 269.
(31) Vaillancourt, F. H.; Barbosa, C. J.; Spiro, T. G.; Bolin, J. T.; Blades, M. W.; Turner, R. F. B.; Eltis, L. D. *J. Am. Chem. Soc.* **2002**, *124*, 2485.
(32) Bolin, J. T.; Eltis, D. In *Handbook of Metalloproteins;* Messerschmidt, A., Huber, R., Poulus, T., Wieghardt, K., Eds.; Wiley: Chichester, 2001; pp 632−642.
(33) Deeth, R. J.; Bugg, T. D. H. *J. Biol. Inorg. Chem.* **2003**, *8*, 409.
(34) Spence, E. L.; Langley, G. J.; Bugg, T. D. H. *J. Am. Chem. Soc.* **1996**, *118*, 8336−8343.

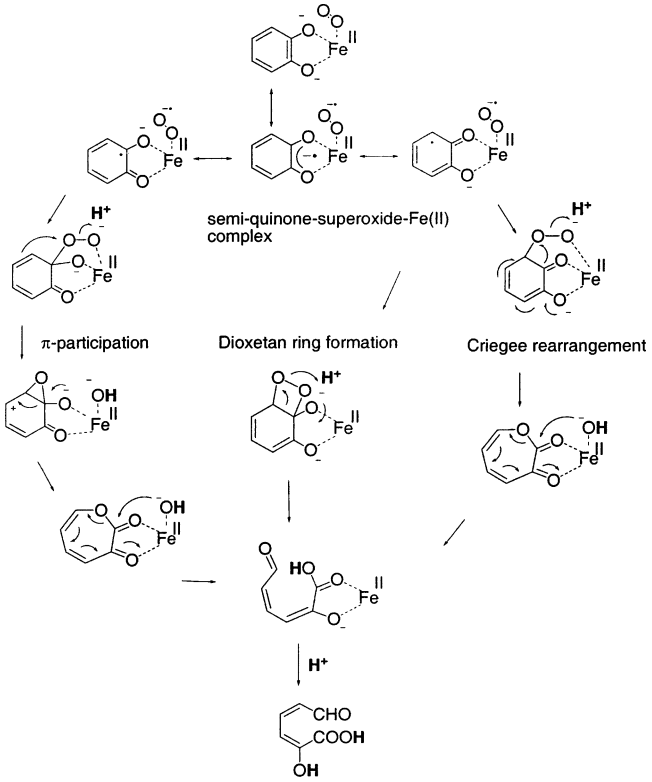

Figure 3. Different mechanisms suggested previously for extradiol dioxygenases.

On the basis of all the available spectroscopic and X-ray crystallographic data collected, several mechanisms of how the extradiol dioxygenases operate have been suggested (see Figure 3). Lipscomb and Que have suggested mechanisms for both the intra- and extradiol dioxygenases.[18,27] In their mechanisms, nucleophilic attack yields a bridged peroxy intermediate followed by Criegee-type rearrangements, where the transition states involve concerted breaking of the O−O and C−C bonds (see Figure 3). Bugg and co-workers have suggested an alternative mechanism,[3,4,34] where they argue that the peroxide, bridging the catechol and the Fe(II) center, is cleaved heterolytically by a nucleophilic attack from the catechol π-system (π-participation), producing an epoxide placed on the now cationic catechol intermediate and a hydroxide ion bound to Fe(II) (see Figure 3). The catechol "extra" C−C bond, being part of the epoxide, subsequently breaks, and the product is released after addition of the Fe(II)-bound hydroxide to the seven-membered lactone ring. Hayaishi et al. suggested a mechanism based on the observation that 2,3-CTD from *Pseudomonas arvilla* incorporated both oxygen atoms of $^{18}O_2$ into the product, involving a dioxetane intermediate (see Figure 3). This mechanism was later ruled out by Sanvoisin et al. using ^{18}O labeling techniques.[35]

One intriguing question which remains unanswered is that of how the intradiol and extradiol dioxygenases selectively catalyze the ring-fission, via cleavage either of the C−C bond between the hydroxyl groups of the catechol or of the C−C bond outside those groups. Bugg and Lin[36] have suggested one way a Criegee-type mechanism could dictate regiospecific cleavage of the C−C bond (intradiol and extradiol cleavage). By assuming that both the intradiol and extradiol dioxygenases cleave the "extra" and "intra" C−C bonds via alkenyl- or acyl-migrating 1,2-shifts (also called Criegee rearrangement when the rearrangement involves an alkyl hydroperoxide[37]), the control of alkenyl or acyl migration could lie in the difference of alignment of the hydroperoxide formed relative to the cyclohexadienone ring (see Figure 3). The extradiol-cleaving catechol dioxygenases with a His_2Glu motif coordinating the Fe(II) ion would position the hydroperoxide in an axial antiperiplanar orientation with respect to the alkenyl group ("extra" C−C bond), allowing for σ-migration (Criegee rearrangement). Alternatively, extradiol cleavage could occur through attack by the C−C π-bond on the O−O bond via π-orbital overlap with the peroxide σ^* orbital. This would put a transient epoxide on the ring ("extra" position) bearing an adjacent allylic carbocation (see Figure 3). Rapid C−C bond cleavage would give the α-keto-lactone. The intradiol-cleaving catechol dioxygenases with a His_2Tyr_2 motif around the Fe(III) ion would constrain the hydroperoxide in a quasi-equatorial position relative to the cyclohexadienone ring, giving instead acyl migration and intradiol cleavage of the catechol ring. Consequently, the difference in the positioning of the hydroperoxide relative to the cyclohexadienone ring and the difference in electronic effects (orbital steering) should affect the subsequent cleavage of the O−O and C−C bonds and would, according to Bugg and Lin, account for the regiospecific cleavage of the C−C bond in catecholic substrates. Their suggested mechanism is, however, based on the assumption that all four residues (His_2Tyr_2) coordinate to the Fe(III) ion of the intradiol catechol dioxygenase enzyme during the C−C bond-cleaving process. However, it is known that the axial tyrosinate (Tyr447) of 3,4-PCD gives up its coordination to Fe(III) when catechol binds and adopts an orientation where it points away from the Fe(III) center.[11] The increased number of possible coordination sites around Fe(III) would then enable the hydroperoxide to adopt a quasi-axial (or quasi-equatorial) position relative to the cyclohexadienone ring, and no discrimination between intra- and extradiol C−C cleavage would result. Bugg and Lin reason that the tyrosine residue, after substrate binding, could swing back toward the Fe(III) center and restrict the positioning of the hydroperoxide relative to the cyclohexadienone ring.

Apart from the first-shell ligands, His146, His210, and Glu260, also the hydrogen-bonding residues Tyr250, His241, and His195 in the second coordination shell are conserved in all extradiol dioxygenases.[32] Several of the first and second solvation shell residues in the extradiol dioxygenases have been replaced by other residues by mutagenesis engineering. A particularly interesting mutation result appeared recently when His195 in an extradiol dioxygenase was mutated to a phenylalanine, which changed the selectivity from extradiol to intradiol cleavage for a substrate analogue.[38] This has many important implications for the mechanism. First, it is not necessary to have an Fe(III) center to perform intradiol cleavage. Second, since His195 is only a second-shell ligand, it appears that the extradiol and intradiol dioxygenases have overall quite similar mechanisms and that the selectivity is determined by subtle details of

(35) Sanvoisin, J.; Langley, G. J.; Bugg, T. D. H. *J. Am. Chem. Soc.* **1995**, *117*, 7836.
(36) Bugg, T. D. H.; Lin, G. *Chem. Commun.* **2001**, 941.
(37) Lowry, T. H.; Richardson, K. S. *Mechanism and Theory in Organic Chemistry*; Harper & Row: New York, 1976; p 327.
(38) Groce, S. L.; Lipscomb, J. D. *J. Am. Chem. Soc.* **2003**, *125*, 11780.

the mechanisms. Many results using biomimetic complexes have pointed in the same direction.[3,39]

Many attempts have been made to achieve extradiol cleavage of catecholic substrates using model systems of the extradiol dioxygenases.[3,39,40] Most of these models have tetradentate ligands, modeling more closely the coordination around Fe(III) in intradiol enzymes. These tetradentate ligands, both when complexed to Fe(II) and Fe(III), catalyze the intradiol degradation of catechols. Only very few ligands, most of them tridentate, give rise to extradiol cleavage products. However, it should be noted that some of these products (pyrones) are derived from loss of CO and therefore may not directly be derived from extradiol cleavage.[3] The reactions require the presence of a base such as pyridine. This suggests that the orientation of a basic residue in the active site of the enzyme, to facilitate proton transfer, plays a central role during the catalysis.

Bugg et al. have demonstrated that Fe(II) and Fe(III) complexes of tridentate ligands catalyze both intra- and extradiol cleavage of the catechol ring.[28,41] However, when the ligands are complexed to Fe(II), the reaction proceeds with higher rate and specificity toward extradiol cleavage. On the basis of this finding, Bugg et al. reasoned that Fe(II) has a higher chemical reactivity for extradiol cleavage than Fe(III).

The mechanisms of how extra- and intradiol dioxygenases activate oxygen and regioselectively cleave the catechol C−C bond are still not fully understood. The wealth of structural and spectroscopic data collected from these enzymes makes them attractive for theoretical investigations. Consequently, we have performed extensive calculations on both the intra- and extradiol dioxygenases over several years, and we would like to present our perspective on the mechanisms of these enzymes. Herein we present an alternative mechanism for the extradiol dioxygenases which agrees well with experimental observations. We have applied a large model system which takes into account both the first and part of the second coordination sphere around the ferrous center. We point out the mechanistic role of the first solvation shell ligands around the ferrous center but also several residues in the second solvation shell.

To better understand the underlying mechanism that controls the regioselective cleavage of the extradiol C−C cleavage, we have studied small model systems in addition to the large enzyme model. These results are presented and discussed in relation to the results obtained from the large model calculations.

II. Computational Details

The calculations were performed in three steps. First, an optimization of the geometry was made using the B3LYP method[42] with double-ζ (lacvp) basis sets. In the second step, the B3LYP energy was evaluated for the optimized geometry using a larger basis set where polarization functions were added (lacv3p*). An effective core potential was used for the iron atom.[43]

To keep the optimized structures close to the experimental ones, some atoms were frozen from their corresponding positions in the X-ray structure.[32] The fixed atoms are marked with an asterisk in the figures below. A fixation procedure is necessary whenever second-shell ligands are included in the model.[44,45] Due to the long computation times, Hessians were computed only for the transition states, which means that zero-point effects are neglected.

In the third step, the surrounding protein was treated with a self-consistent reaction field method, using a Poisson−Boltzmann solver. The dielectric constant of the homogeneous dielectric medium was set equal to 4.0, in line with previous modelings of enzymes.[46] The probe radius was set to 2.50 Å to avoid artifacts sometimes encountered using a smaller radius. No geometry optimizations including the dielectric continuum were made since the calculated dielectric effects were found to be quite small. The calculations can thus be written in short-hand notation as B3LYP/lacv3p* energies, including solvent contributions based on B3LYP/lacvp geometries. Most geometry optimizations were carried out using the Jaguar program,[47] while the Hessians and transition-state optimizations were made with the GAUSSIAN-98 program.[48] The experience and accuracy obtained for the present type of calculations for redox-active enzymes can be found in recent reviews.[45,49−52]

Since the most recent high-accuracy study of the mechanism of an extradiol dioxygenase was made using the BP86 functional,[33] it could be of interest to compare the accuracy of B3LYP to nonhybrid methods such as BP86. Benchmark tests for first- and second-row elements consistently show hybrid DFT methods such as B3LYP to be considerably more accurate for energetics than nonhybrid methods such as BP86. For the 55 G2 molecules, the mean absolute deviation of B3LYP is 2.20 kcal/mol, while that of BP86 is 10.32 kcal/mol.[53] For the 376 entries in the G3/99 benchmark test,[54] the mean absolute deviation for B3LYP is 4.27 kcal/mol, while the one for the nonhybrid BLYP functional is 7.60 kcal/mol. Excluding the 75 largest molecules (G2/97), B3LYP gives 3.29 kcal/mol and BLYP 6.17 kcal/mol. For metal complexes of the first transition row, benchmark tests do not exist due to the lack of a sufficient number of accurate experimental results. For the comparisons that have been made to the known experimental results, B3LYP has again been found to be clearly superior to BP86, at least for the right-hand-side of this transition row.[45,49,50] An example with a large deviation between the different functionals is the O−H bond strength of the permanganate ion, $MnO_3(OH)^-$, which has been measured to be 80 ± 3 kcal/mol.[55] In this case, B3LYP gives 77.2 kcal/mol and BP86 gives 60.6 kcal/mol, a deviation of 20 kcal/mol from experiments.

(39) Que, L., Jr.; Kolanczyk, R. C.; White, L. S. *J. Am. Chem. Soc.* **1987**, *109*, 5373−5380.
(40) Jo, D. H.; Que, L., Jr. *Angew. Chem., Intl. Ed.* **2000**, *39*, 4284.
(41) Lin, G.; Reid, G.; Bugg, T. D. H. *J. Chem. Soc., Chem. Commun.* **2000**, 1119−1120.
(42) Becke, A. D. *Phys. Rev.* **1988**, *A38*, 3098; *J. Chem. Phys.* **1993** *98* 1372; *J. Chem. Phys.* **1993**, *98*, 5648.
(43) Hay, P. J.; Wadt, W. R. *J. Chem. Phys.* **1985**, *82*, 299.
(44) Pelmenschikov, V.; Blomberg, M. R. A.; Siegbahn, P. E. M. *J. Biol. Inorg. Chem.* **2002**, *7*, 284−298.
(45) Siegbahn, P. E. M. *Q. Rev. Biophys.* **2003**, *36*, 91−145.
(46) Blomberg, M. R. A.; Siegbahn, P. E. M.; Babcock, G. T. *J. Am. Chem. Soc.* **1998**, *120*, 8812−8824.
(47) Jaguar 4.0, Schrödinger, Inc., Portland, OR, 1991−2000.
(48) Frisch, M. J.; Trucks, G. W.; Schlegel, H. B.; Scuseria, G. E.; Robb, M. A.; Cheeseman, J. R.; Zakrzewski, V. G.; Montgomery, J. A., Jr.; Stratmann, R. E.; Burant, J. C.; Dapprich, S.; Millan, J. M.; Daniels, A. D.; Kudin, K. N.; Strain, M. C.; Farkas, O.; Tomasi, J.; Barone, V.; Cossi, M.; Cammi, R.; Mennucci, B.; Pomelli, C.; Adamo, C.; Clifford, S.; Ochterski, J.; Petersson, G. A.; Ayala, P. Y.; Cui, Q.; Morokuma, K.; Malick, D. K.; Rabuck, A. D.; Raghavachari, K.; Foresman, J. B.; Cioslowski, J.; Ortiz, J. V.; Stefanov, B. B.; Liu, G.; Liashenko, A.; Piskorz, P.; Komaromi, I.; Gomperts, R.; Martin, R. L.; Fox, D. J.; Keith, T.; Al-Laham, M. A.; Peng, C. Y.; Nanayakkara, A.; Gonzalez, C.; Challacombe, M.; Gill, P. M. W.; Johnson, B.; Chen, W.; Wong, M. W.; Andres, J. L.; Head-Gordon, M.; Replogle, E. S.; Pople, J. A. *Gaussian 98*; Gaussian Inc.: Pittsburgh, PA, 1998.
(49) Siegbahn, P. E. M.; Blomberg, M. R. A. *Annu. Rev. Phys. Chem.* **1999**, *50*, 221−249.
(50) Siegbahn, P. E. M.; Blomberg, M. R. A. *Chem. Rev.* **2000**, *100*, 421−437.
(51) Blomberg, M. R. A.; Siegbahn, P. E. M. *J. Phys. Chem. B* **2001**, *105*, 9375−9386.
(52) Himo, F.; Siegbahn, P. E. M. *Chem. Rev.* **2003**, *103*, 2421−2456.
(53) Bauschlicher, C. W., Jr.; Ricca, A.; Partridge, H.; Langhoff, S. R. In *Recent Advances in Density Functional Methods, Part II*; Chong, D. P., Ed.; World Scientific Publishing Co.: Singapore, 1997; p 165.
(54) Curtiss, L. A.; Raghavachari, K.; Redfern, P. C.; Pople, J. A. *J. Chem. Phys.* **2000**, *112*, 7374−7383.
(55) Gardner, K. A.; Kuehnert, L. L.; Mayer, J. M. *Inorg. Chem.* **1997**, *36*, 2069−2078.

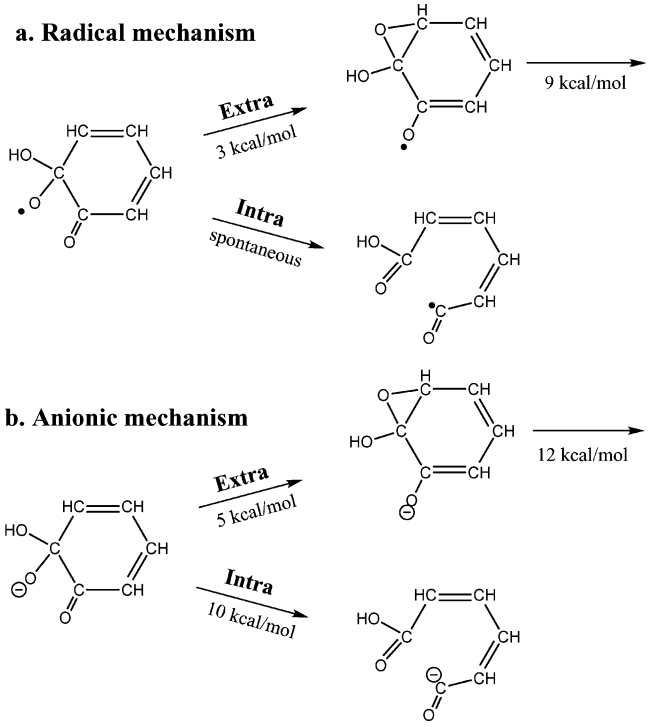

Figure 4. Radical (a) and anionic (b) mechanisms for extra- and intradiol C−C bond cleavage for the oxidized substrate. The energies refer to barriers.

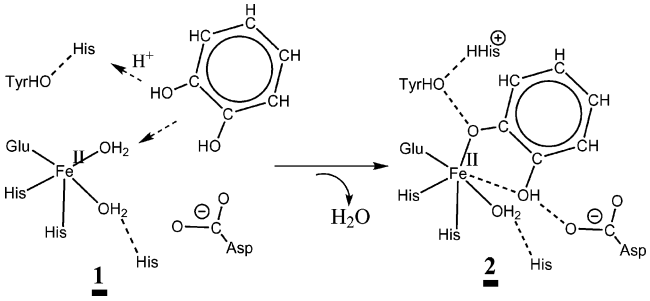

Figure 5. Catechol binding in the suggested mechanism for extradiol dioxygenase.

III. Results and Discussion

Over the past years, a large number of calculations have been made in our group to study the mechanism of extradiol dioxygenase and also the corresponding mechanism of cleavage of intradiol dioxygenase. Several models have been used, ranging from 20 atoms to the present model with about 70 atoms. Most of the findings for the smaller models have been incorporated into the study of the present model, and the discussion below will therefore focus on the results of the most recent model. In this model, experimentally known structural features have been carefully built in, such as the known position of the catechol substrate and the experimentally suggested position for dioxygen. The amino acids at the active site, implied to be most significant for the substrate mechanism, have been included in the model. These residues include His146, His210, and Glu260 in the first coordination shell and His195, His241, Asp244, and Tyr250 in the second shell. The histidines are, as usual, modeled by imidazoles, and the aspartates and glutamates are modeled as formates. Since the second-shell tyrosine ligand is expected to act as a mediator only for protons being transferred from the complex, it was considered sufficient to model it as a water molecule. In the optimizations, one position of each amino acid residue was fixed from the corresponding position in the X-ray structure, except for His241, where two positions had to be fixed in order to avoid too large movements.

Before the actual mechanism of extradiol dioxygenase is discussed, some model results for the oxy-substrate itself, of key significance for the selectivity, should be mentioned. Two types of mechanisms will be discussed below, a radical mechanism and an anionic mechanism, and two pathways for C−C bond cleavage, intradiol cleavage and extradiol cleavage (see Figure 4). These simple models were chosen as likely products after oxidation of the substrate. The calculations were performed at the B3LYP/6-31+G* level including zero-point energies. The model results can be described as follows. For the radical mechanism, intradiol cleavage occurs spontaneously in the optimization. "Extra" epoxide formation is less preferred, with a barrier of 3 kcal/mol. From the "extra" epoxide, extradiol bond cleavage occurs with a barrier of 9 kcal/mol. For the anionic mechanism, "extra" epoxide formation occurs with a barrier of 5 kcal/mol, while intradiol cleavage has a barrier of 10 kcal/mol. It therefore seems that the "extra" pathway is preferred for the anion. However, a complicating factor is that the extradiol C−C bond cleavage from the anionic epoxide has a barrier of 12 kcal/mol, which is actually higher than that for the intradiol C−C bond cleavage. In this context, it is interesting to note that a radical anion (obtained by removing the hydroxyl hydrogen atom) of the "extra" epoxide actually opens up spontaneously. In summary, if the enzyme can produce an oxy-substrate radical, intradiol cleavage is likely to be preferred. If, instead, an oxy-substrate anion is produced, "extra" epoxide formation will be preferred, but the pathway from this point onward would be unclear if the system remains an anion. If the "extra" epoxide would change toward a radical, the "extra" epoxide would open spontaneously. This type of pathway is actually very close to that found below for the model of the extradiol dioxygenases.

a. Binding of Catechol. The first structure studied, relevant for the mechanism of extradiol dioxygenase, is the result of binding of the catechol substrate to the Fe(II) complex (see Figure 5). An X-ray structure of this complex exists (see Figure 2), and the corresponding optimized structure is shown in Figure 6. Four different protonation states were studied, and the one found to have the lowest energy is shown in the figure. This structure has the catechol bound as a monoanion, in agreement with experimental interpretations.[1] The proton removed from catechol has moved to His241 over Tyr250. The proton on the second OH group of the catechol still prefers to stay on catechol. Keeping both protons on catechol is 5.3 kcal/mol higher in energy (using a slightly smaller model without His 195), and removing both protons of catechol, leading to a dianionic substrate, is 1.8 kcal/mol higher in energy. In that case, the second proton removed was placed on Asp244. While the protonation state at this stage bears some relevance for the mechanism, its role should not be overinterpreted, since the energy differences to other protonation states are rather small in the context of the entire mechanism, involving the cleavage of the O−O bond of dioxygen, for example. However, what is important is that both of the catechol protons are easily available for the catalytic chemistry.

The optimized distances compare fairly well to those of the X-ray structure. The distances between iron and His210 and

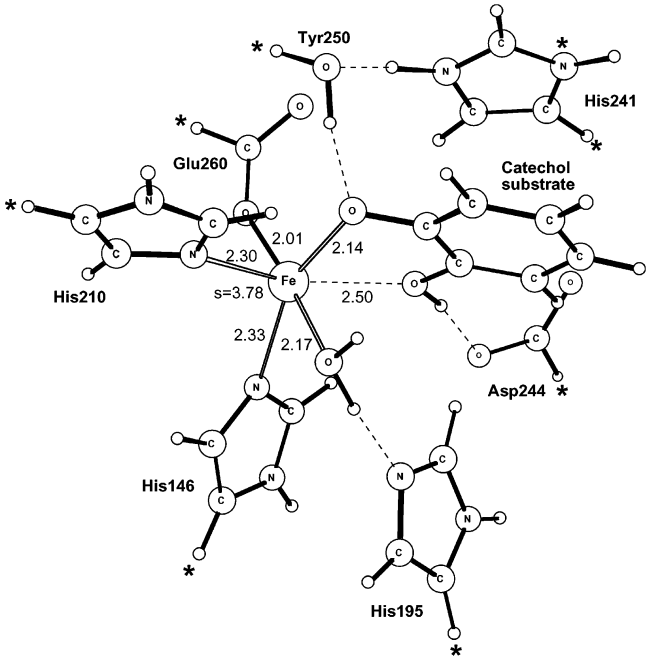

Figure 6. Fully optimized structure of the reactant with complexed catechol. Atoms marked with an asterisk were frozen from the X-ray structure. Distances are given in angstroms, and spins larger than 0.10 are given.

Glu260 agree very well, while the distances from iron to His146, catechol, and water deviate by 0.1−0.2 Å. With the normal errors in an X-ray structure resolved to 1.9 Å,[12] it is questionable if the deviations from the optimized distances can be concluded to be numerically significant. The differences could also be due to a minor basis set problem, since rather small basis sets were used in the optimization. Still, this basis set has been shown in numerous studies to be quite sufficient for the energetics. The spin population of iron is 3.78, which is typical for Fe(II). The remaining, small spin population of 0.22 is spread out on all the first-shell ligands.

A few comments should be made on the binding of the water to Fe(II), since in two recent studies it has been suggested that water does not bind to iron at this stage.[13,14] This finding is actually not in disagreement with the present results. For a model without His195, the binding energy for water was found to be 10.5 kcal/mol. This rather small binding energy should be compared to the entropy gained if water does not bind to iron, which should be on the same order. Alternatively, when water is released from iron, it would find a position with hydrogen bonds that should also amount to a similar energy. For the present study, it would therefore not make a significant energetic difference if water is bound to iron at this stage or not.

b. Binding of Dioxygen. The next step of the mechanism is the binding of dioxygen to the metal. There is no X-ray structure of any dioxygen-bound complex for this enzyme, but there is a structure with bound NO.[13] This structure shows that NO binds equatorially, replacing the water ligand. It should be noted that this position for binding O_2 differs from the assumption made in the previous DFT investigation, where dioxygen was placed trans to His146, which requires a reorientation of the catechol substrate from its position in the X-ray structure in Figure 2. In the optimal structure of the present study, with dioxygen trans to Glu260, the water being displaced keeps its hydrogen bond to His195. At the same time, the proton on the nearest catechol oxygen is transferred to Asp244, which reorients and forms a

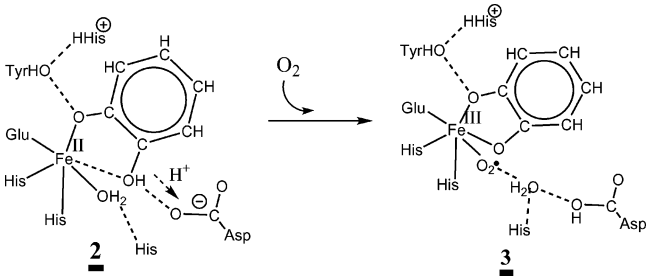

Figure 7. Dioxygen binding in the suggested mechanism for extradiol dioxygenase.

hydrogen bond to the water, as shown in Figure 7. This type of structure was reached after a number of investigations using smaller models. Still, it is clear that other, more favorable possibilities cannot be excluded. One of many structures tried had the catechol proton transferred to His195 stabilized by an interaction with the anionic Asp244, but this type of structure was found to be slightly less favorable. There are two significant points that should be noted for structure **3**. First, it is important for the binding energy of O_2 that a hydrogen bond is formed, since O_2 becomes anionic. In many other enzymes studied recently, a similar strategy, using the displaced water for hydrogen-bonding purposes, has been adapted by the enzyme for obtaining a sufficient binding energy for dioxygen and probably occurs quite widely. Second, the preferred hydrogen bond is to the oxygen directly bound to iron, which has consequences for the product of the subsequent O−O bond cleavage. The main possible spin states for the type of structure in Figure 7 were optimized. Two of them are of particular interest for the mechanism. The septet state ($S = 3$) was found to be lowest in energy. The spin populations for this state indicate that the electronic structure is best described as a mixture of two reference configurations. The spin on iron is 4.04, which is between those typical for Fe(II) and Fe(III): the spin on catechol is 0.67, and that on dioxygen is 1.12. One of the reference configurations should thus have an Fe(III) oxidation state and a superoxo radical with its spin parallel to the one on iron. The second reference configuration should also have a superoxo radical but an Fe(II) oxidation state and a catechol radical, with all spins parallel. This septet state is 3.4 kcal/mol more stable than the reactant in Figure 6, with dioxygen in the second shell. It should be noted that entropy effects have not been determined, since these cannot be reliably obtained for structures where some atoms are fixed. With entropy effects added, the dioxygen structure is undoubtedly less stable than the reactant with free dioxygen, perhaps by as much as 5 kcal/mol. This estimate includes the possibility that water is actually not bound to iron at the stage when dioxygen binds[13,14] (see above). The endergonic binding of dioxygen is quite general for the present type of complexes and is the reason so few dioxygen complexes have been crystallized. The finding that dioxygen binding is endergonic also agrees with the experimental observation that dioxygenases in the resting ferrous state, in the absence of substrate, are not highly reactive toward dioxygen, even though they are only five-coordinated.[2] The second lowest state found is the quintet ($S = 2$). This state is particularly interesting for the mechanism and is therefore shown in Figure 8. This state has a clear Fe(II) oxidation state with both a peroxo and a catechol radical. The spin on iron is 3.86 (close to that of the Fe(II) reactant in Figure 6), the spin on

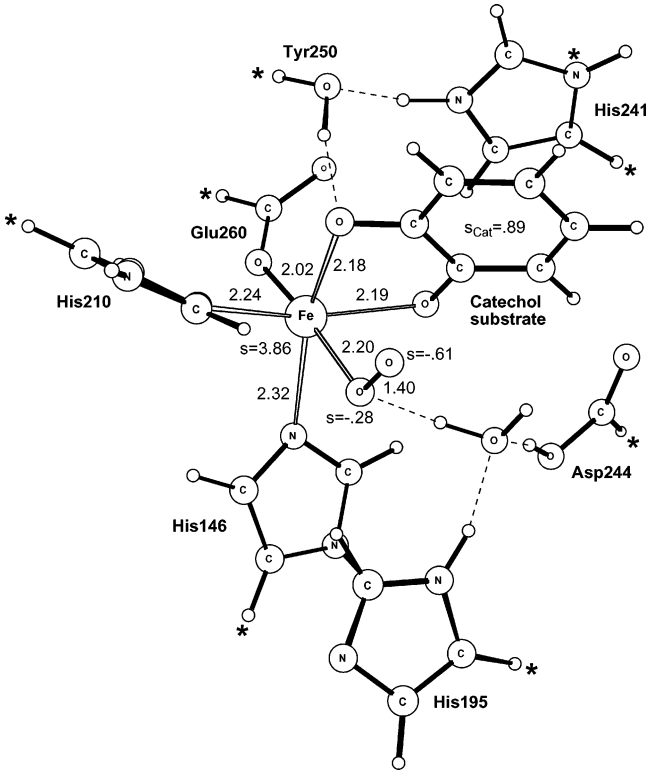

Figure 8. Fully optimized structure of the quintet reactant with catechol and dioxygen. Atoms marked with an asterisk were frozen from the X-ray structure. Distances are given in angstroms, and spins larger than 0.10 are given.

dioxygen is −0.89, and the spin on catechol is +0.89. The energy of the quintet state is 5.5 kcal/mol higher than that of the septet state, but the quintet state is the natural precursor for the next step of the mechanism. Both the quintet and the septet states correspond rather well to the binding state of dioxygen predicted by experiments.[18,27,34]

It is difficult to compare our results with the DFT results of Davis et al.,[14] since the substrate-free active site was not studied and they did not study the catalytic reaction. Furthermore, very few details of their results were given. The geometry obtained at the B3LYP level appears to be reasonably similar in the two studies. In the study by Davis et al., a few explanations were given for the increased reactivity of the substrate-bound complex with dioxygen compared to that when the substrate is not bound: (1) substrate binding may lower the redox potential by enhancing the stability of the ferric ion; (2) the trans effect of the stronger axial ligand could increase the interaction with acceptors such as O_2 or more favorably orient the redox-active orbital; (3) the protein environment is better able to stabilize Fe(III)−O_2^-; and (4) the substrate can allow two-electron reduction of O_2, which is more favorable than the one-electron chemistry. While the present results agree with most of these conclusions, the present explanation for the difference of the reactivity of dioxygen with and without bound substrate is even simpler, namely that this process is endergonic for the substrate-free case. When the substrate enters, dioxygen binding is still endergonic, but catalysis can start, which is exergonic. This scenario has been found to be the same for all non-heme enzyme complexes studied by DFT so far: phenyl alanine hydroxylase, α-ketoglutarate-dependent enzymes, and naphthalene dioxygenase.[56−58]

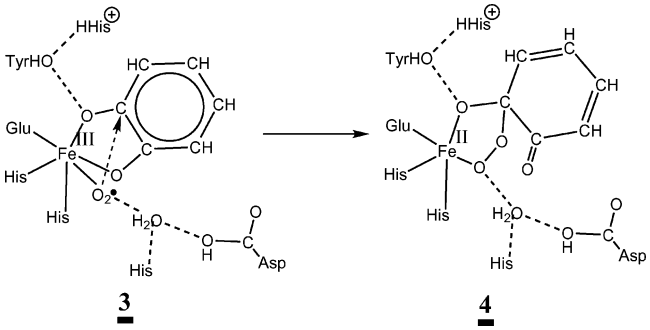

Figure 9. Peroxide attack on the substrate in the suggested mechanism for extradiol dioxygenase.

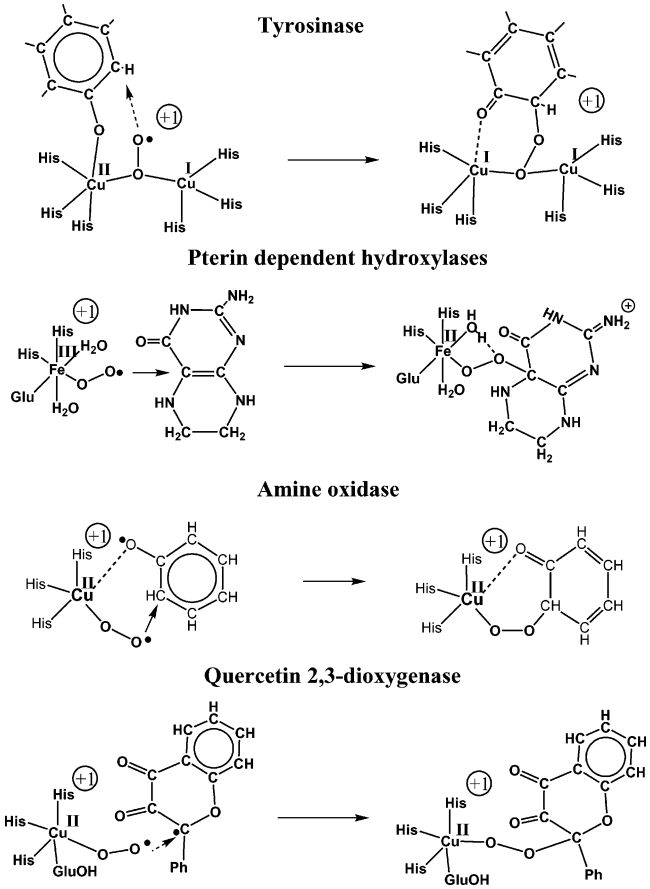

Figure 10. Peroxide attack on substrates in different enzymes.

c. Superoxo Radical Attack on Catechol. This step is one of the two most important events in the catalytic cycle (see Figure 9). It is also a common step for many enzymes studied recently by similar theoretical techniques (see Figure 10). For all these enzymes, dioxygen first binds directly to the metal, mostly as a peroxo radical and most of the time displacing a water molecule. To prepare for the attack, the substrate then has to be excited to a state where the substrate is a radical and where the spin on the substrate has the direction opposite to the one on the superoxo radical. As discussed above, this excitation costs 5.5 kcal/mol for the extradiol dioxygenase;

(56) Bassan, A.; Blomberg, M. R. A.; Siegbahn, P. E. M. *Chem. Eur. J.* **2003**, *9* 106−115.
(57) Borowski, T.; Bassan, A.; Siegbahn, P. E. M. *Chem. Eur. J.* **2004**, *10* 1031−1041.
(58) Bassan, A.; Blomberg, M. R. A.; Siegbahn, P. E. M. *J. Biol. Inorg. Chem.*, in press.

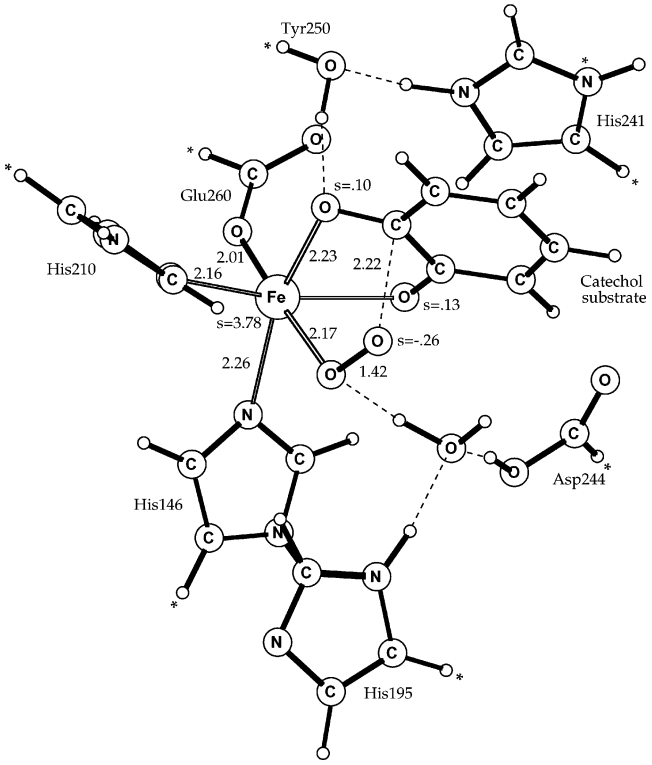

Figure 11. Fully optimized transition-state structure for peroxide bridge formation in extradiol dioxygenase. Atoms marked with an asterisk were frozen from the X-ray structure. Distances are given in angstroms, and spins larger than 0.10 are given.

similarly, there is an excitation required in tyrosinase.[59] In pterin-dependent amino acid hydroxylases, the excitation energy is close to zero,[56] while in other enzymes, it is actually zero since the substrate radical state is the ground state. This is the case for the biogenesis of the TPQ cofactor in amine oxidase[60] and for the substrate reaction in quercetin dioxygenase,[61] for example.

With dioxygen and the substrate prepared as radicals, the formation of a bridging peroxide is quite facile. There are essentially two possibilities, an attack either on the C−O carbon closest to Tyr250, as shown in Figure 9, or on the other carbonyl carbon. The other catechol carbons are too far away from the peroxy radical. The C−O group which is not under attack will form a C═O double bond in this process (see Figure 9). This will favor attack on the C−O group which has a hydrogen bond to Tyr250, since in this case no hydrogen bond will be disrupted. The fully optimized quintet transition state (TS) for this attack is shown in Figure 11. The computed barrier with respect to the septet reactant is 8.5 kcal/mol, and with respect to the quintet precursor it is only 3.0 kcal/mol. The imaginary frequency is rather low, at 195 cm^{-1}, since no hydrogen motion is involved. The critical C−O distance at the TS is 2.22 Å, indicating an early reaction. The spins (absolute values) on both the superoxo and the catechol parts have decreased from their values for the quintet precursor, down to −0.35 for superoxo and 0.47 for the catechol. For the quintet product with a bridging peroxide, these spins are almost entirely quenched. The spin on iron stays almost exactly the same from the quintet precursor: 3.86 for the

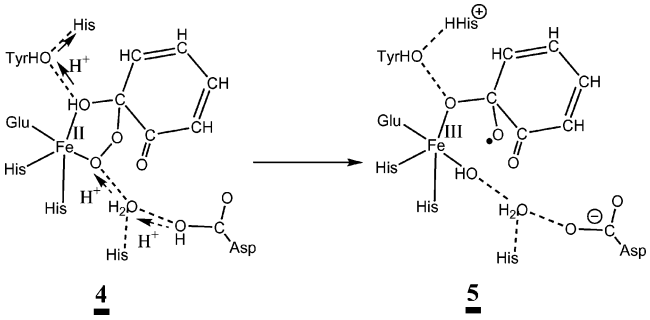

4 **5**

Figure 12. O−O bond cleavage step in the suggested mechanism for extradiol dioxygenase.

precursor, 3.78 at the TS, and 3.78 for the product. The reaction is almost thermoneutral (−0.3 kcal/mol) with respect to the quintet precursor and is endothermic by 5.2 kcal/mol with respect to the septet reactant. The attack of a peroxy radical with formation of a bridging peroxide is in agreement with most mechanisms suggested for the extradiol dioxygenases on the basis of experiments.[3,4,18,27,34]

For each intermediate in the presently suggested mechanism, it has been tested whether the proton on His241 would like to go back to the catechol substrate. The peroxo-bridging intermediate **4** is the only one where this turned out to be the case. Since the oxygen at the sp^3-hybridized carbon on the catechol is quite negative, the proton prefers to go back from His241 by 4.1 kcal/mol. As a comparison, for the precursor **3** the proton prefers to be on His241 by 8.1 kcal/mol and for the TS by 8.4 kcal/mol. Dielectric effects are quite important for this large difference, increasing it by 5.6 kcal/mol (from 2.5 to 8.1 kcal/mol) and 4.0 kcal/mol, respectively. With an energy-lowering effect of 4.1 kcal/mol for the peroxide product, this step changes from being endothermic by 5.2 kcal/mol to being endothermic by 1.1 kcal/mol with respect to the septet reactant.

Another test which was made for each intermediate was whether the proton on Asp244 instead would prefer to be on His195, but this was never found to be the case. For example, for the TS of this step, the preference for the proton to be at Asp244 is 4.2 kcal/mol. The large basis set is important for establishing this difference, changing it from −4.9 to +4.2 kcal/mol. The proton on Asp244 does not want to be moved to the peroxide, either, at this stage. These results do not necessarily mean that the proton will not reside on His195 if a still larger model was used. For example, a model including also His194 and Asp171 (which are hydrogen-bonded in a chain with His195) might stabilize the protonated His195 sufficiently to change the situation somewhat. However, it is not likely that this would be a major effect and change the present mechanism significantly.

d. O−O Bond Cleavage. In the first event in the next step, the proton on the substrate moves back to His241. This step is mechanistically not very significant but occurs since the energy at the transition state for O−O bond cleavage is lower with the proton on His241. In contrast, another proton transfer is very important in order to obtain a reasonable barrier for the O−O bond cleavage: the protonation of the peroxide. This occurs from Asp244 over the water molecule and is concerted with the O−O bond cleavage (see Figure 12). All attempts to cleave the O−O bond without protonating the peroxide led to very high barriers. This conclusion is in line with a similar conclusion

(59) Siegbahn, P. E. M. *J. Biol. Inorg. Chem.* **2003**, *8*, 567−576.
(60) Prabhakar, R.; Siegbahn, P. E. M. *J. Am. Chem. Soc.*, in press.
(61) Siegbahn, P. E. M., submitted.

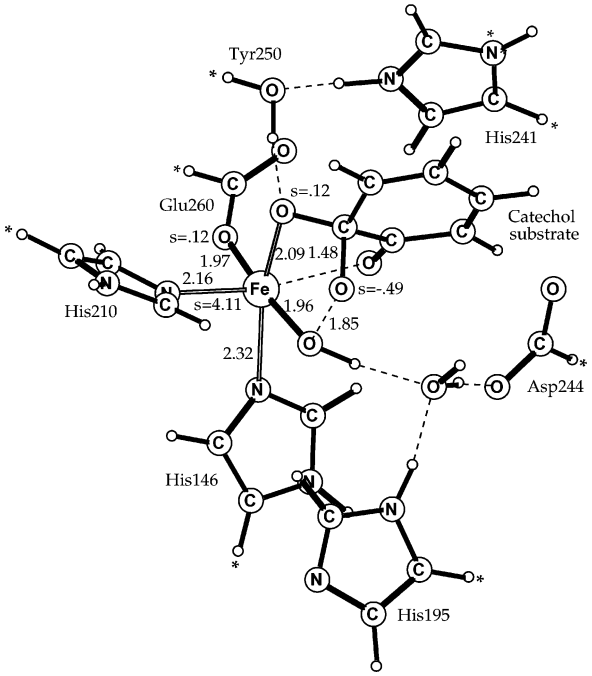

Figure 13. Fully optimized transition-state structure for O−O bond cleavage in extradiol dioxygenase. Atoms marked with an asterisk were frozen from the X-ray structure. Distances are given in angstroms, and spins larger than 0.10 are given.

drawn in the previous DFT study by Deeth and Bugg,[33] but in that case the proton came from Glu260 since the dioxygen was chosen to bind in a position different from the one in the present study. The question is only that of which oxygen of the peroxide should be protonated. In the present model, it was found to be much more favorable to protonate the oxygen directly bound to iron (the inner oxygen). In fact, trying to force the proton to go to the outer oxygen at the TS led back to a protonation of the inner oxygen. The fully optimized TS is shown in Figure 13, which has an imaginary frequency of 301 cm^{-1}. This TS is one of an essentially homolytic cleavage, as evidenced by the large spin-population of −0.49 on the outer oxygen. Iron becomes oxidized to Fe(III). The barrier from the bridging peroxide is 13.9 kcal/mol. Dielectric effects lower the barrier by 3.2 kcal/mol, which is a larger effect than usual but still not very large.

It is interesting to compare this cleavage to the one in pterin-dependent hydroxylases (see Figure 14). In that case, protonation of the outer oxygen is sterically forced as the result of a water molecule being coordinated to iron as proton donor, and instead leads to the formation of an Fe(IV)═O species. Which oxygen of the peroxide becomes protonated is thus also very important for the subsequent chemistry.

The O−O bond cleavage is endothermic by 8.4 kcal/mol from the starting point with the proton on the substrate rather than on His241. The detailed structure of the product, shown in Figure 15, determines the selectivity of the enzyme. As can be seen in the figure, the oxygen derived from the peroxide has a large spin of −0.68. However, the total spin-population of the catechol is less than that, at −0.48. The charge of the catechol is −0.59, indicating substantial anionic character. This can be compared to the results of the parallel study of the intradiol enzyme, where the catechol obtains a spin of −0.70 and a charge of −0.41, indicating a more radical species. This difference,

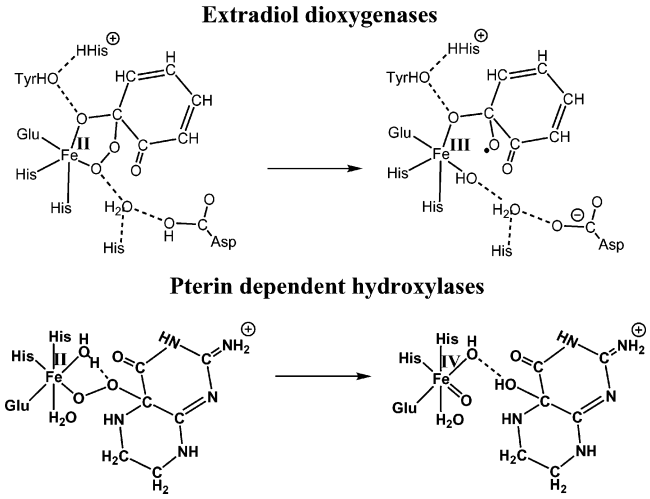

Figure 14. O−O bond cleavage in extradiol dioxygenases and pterin-dependent hydroxylases.

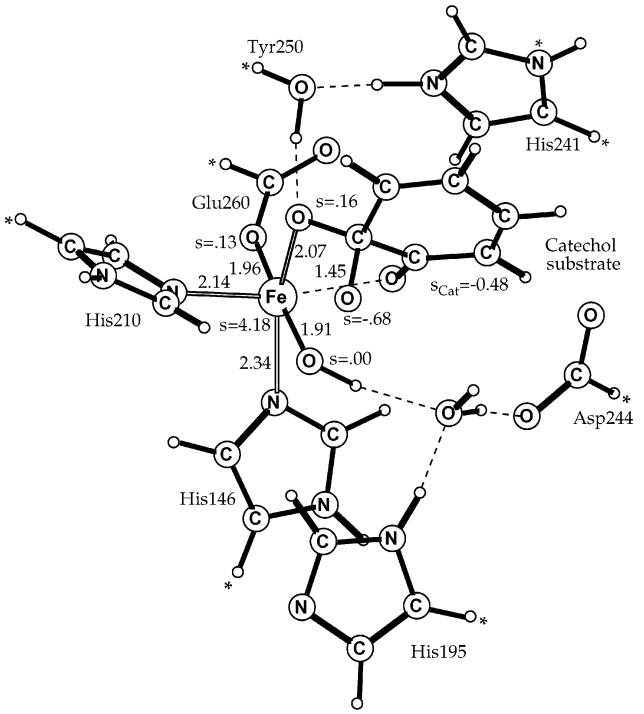

Figure 15. Optimized structure for the intermediate radical in extradiol dioxygenase. Atoms marked with an asterisk were frozen from the X-ray structure. Distances are given in angstroms, and spins larger than 0.10 are given.

although apparently rather small, turns out to be important for the different selectivities of the enzymes. The spin on iron for the O−O cleavage product is 4.18, characteristic for Fe(III), as expected. It should finally be noted that, in the presently suggested mechanism, the O−O bond is cleaved prior to the C−C bond. However, as will be shown below, the extradiol C−C cleavage will occur essentially without barrier after the O−O bond is cleaved. In analogy to a similar two-step mechanism for the P450 enzymes, this could be termed a concerted but *nonsynchronous* cleavage of the O−O and C−C bonds. The conclusion drawn from several types of models is that no TS where the O−O and C−C bonds are cleaved simultaneously exists for the present methods and models, and therefore no direct comparison can be made to the TS in Figure

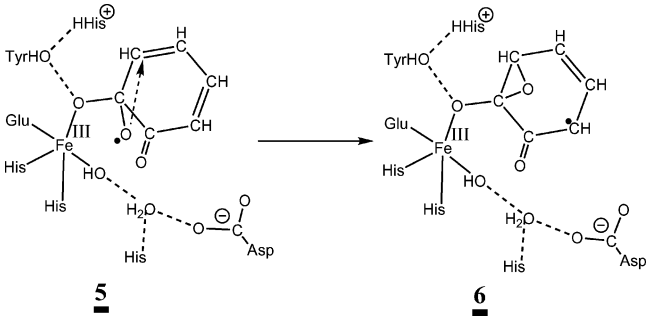

Figure 16. "Extra" epoxide formation in the suggested mechanism for extradiol dioxygenase.

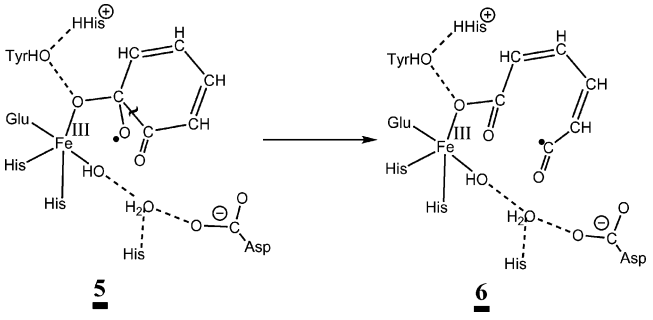

Figure 17. Intradiol ring opening.

13. However, a few single-point calculations with frozen O−O and C−C distances have been done to illustrate how the energy changes. The O−O bond distance is then frozen to the value it has (1.85 Å) in the optimized TS in Figure 13. For a C−C distance frozen to 1.70 Å, the energy is 7.8 kcal/mol higher than it is in the TS in Figure 12, and for C−C = 1.90 Å, it is 22.2 kcal/mol higher. There is no tendency for a second TS, as expected.

e. Formation of the Extra Epoxide. From the intermediate in Figure 15, there are two possible mechanisms for cleaving a C−C bond, and for each one of these there are two different pathways, as shown for the substrate in Figure 4. Step 5 of the extradiol mechanism is shown in Figure 16. The location of the TS for "extra" epoxide formation was done as usual, by a stepwise search following a reaction coordinate optimizing all other degrees of freedom. This led to an approximate TS with a C−O distance to the distant carbon of 1.90 Å and a barrier, using the small basis set, of 4.5 kcal/mol. When the large basis set was used, the barrier decreased to 1.1 kcal/mol. Adding also dielectric effects reduced the barrier to 0.2 kcal/mol only. It is therefore concluded that the barrier for "extra" epoxide formation is essentially zero, to the accuracy of the present methods and models. This result agrees with the findings of Deeth and Bugg[33] but differs on the character of the mechanism. While the present mechanism is dominantly radical, their mechanism was mainly anionic, undoubtedly due to the different DFT functional used. As discussed in section II, in benchmark tests hybrid functionals of the present type in general give more reliable results. The spin on the substrate is −0.76 at the TS, indicating a mainly radical pathway. Also, the present "extra" epoxide product is dominantly radical, in contrast to what was found in the previous study. The spin on the substrate is −0.85, with the spins strongly delocalized over the ring. The overall spin on the substrate is thus significantly larger for the product than for the reactant, which had a spin of −0.59. This change of radical character is also important for the selectivity. As discussed above for the isolated substrate, an anionic epoxide would have a rather large barrier for cleaving the C−C bond, while a radical epoxide opens up more easily. To obtain an optimal extradiol cleavage, a partly radical, partly anionic direct product of the O−O bond cleavage is thus needed which changes to become a cleaner radical as the epoxide is formed. To obtain an optimal intradiol cleavage, all that is needed is to obtain a radical product for the O−O bond cleavage. These findings are in line with the conclusion that intradiol bond cleavage appears to be the kinetically favored pathway under most conditions, based on experimental biomimetic modeling studies.[3]

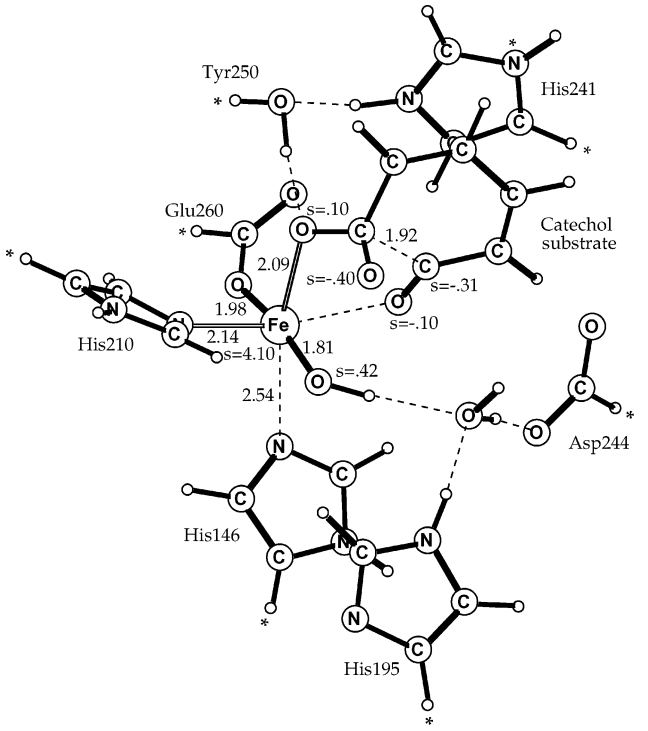

Figure 18. Fully optimized transition-state structure for intradiol bond cleavage of catechol in extradiol dioxygenase. Atoms marked with an asterisk were frozen from the X-ray structure. Distances are given in angstroms, and spins larger than 0.10 are given. Optimization was done using the larger lacvp* basis set.

For a large number of models used in the present study, both the extra- and intradiol cleavages were found to occur with small barriers. This was the case when the product of the O−O bond cleavage was a radical. It is therefore of high importance to investigate both of these pathways to decide which is the preferred one. This was not done in the previous DFT study.[33] In the present study, the most interesting result actually appeared for the intradiol cleavage (see Figure 17), even though this is an extradiol dioxygenase. In the usual stepwise search along a reaction coordinate, an approximate TS was located using the small basis set. This structure was used to fully optimize a TS which led to a barrier of 13.6 kcal/mol, still using the small basis set. However, using the large lacv3p* basis set in this TS led to a decrease of the barrier to 5.0 kcal/mol, an unusually large effect. Furthermore, adding dielectric effects reduced the barrier to 2.6 kcal/mol. Since the effect of using a large basis set was so large, the TS structure was fully reoptimized using a larger lacvp* basis set (see Figure 18). Also, reoptimizing the radical reactant with this basis set and calculating the energy difference using the large lacv3p* basis led to a barrier of 5.9

kcal/mol. Adding dielectric effects led to a final barrier of 4.3 kcal/mol. Zero-point effects are expected to be small since no hydrogen motion is involved at the TS, and the time-consuming calculation of a Hessian for the reactant was therefore not performed, considering also the limitations of the present methods and models anyway. The spin on catechol at the TS is −0.81, indicating a slightly more radical pathway than that for the extradiol cleavage. The spin on iron is slightly reduced to 4.10, still characteristic of Fe(III).

With a computed selectivity in agreement with experiments, an interesting remaining question is that of what features of the extradiol dioxygenase active site are particularly important for the selectivity. The key problems are to avoid formation of Fe(IV) and formation of a clean radical on the substrate. The first question has already been discussed and shown to be mainly dictated by the hydrogen bonding to the oxygen closest to iron (see Figure 14). To see what is important for avoiding the formation of a radical is more difficult. A few decades ago, a more detailed investigation of the reasons for the selectivity would have started with an orbital analysis, or perhaps an energy decomposition. With the higher computer capacity available today, an alternative approach is possible. This approach is similar to what is done in mutation experiments, but it is computationally more convenient to remove rather than replace different amino acids in the surrounding. This was therefore done for each one of the second-shell residues in the model by recalculating the intradiol barrier, keeping the same general mechanism and protonation state. This analysis gave a very clear answer: the only residue with a significant effect on the intradiol barrier is the protonated His241. When the protonated His241 is removed, the barrier for intradiol cleavage becomes zero, and this pathway will therefore be preferred. A similar effect was obtained by removing just the proton. The conclusion is that the protonated, positive His241 draws negative charge over to the substrate. These results were, in fact, very important for realizing that the anionic charge on the substrate plays a key role, as already discussed above. This is a necessary property for obtaining a nonzero barrier for intradiol cleavage.

An interesting experiment in connection with the selectivity of the extradiol dioxygenases was recently reported.[38] It was shown that, when His195 was replaced by a phenylalanine, the selectivity changed from extra- to intradiol cleavage for a substrate analogue. Most importantly, this showed that the difference in the preference for extra- and intradiol cleavage is quite subtle, in agreement with the present mechanism. To reproduce the experimental result would require a separate study, but a plausible reason for the experimental outcome is that the mutation changed the protonation state such that the substrate became more radical.

f. Final Steps. The remaining steps of the catalytic cycle will be described only briefly. The first step after the "extra" epoxide formation is the extradiol C−C bond cleavage, leading to a seven-membered ring (see Figure 19). This step has a low barrier, calculated using the small basis set, which disappears when calculated with the large basis set. Dielectric effects are insignificant. This step is very exothermic by 27.8 kcal/mol, leading to the formation of a seven-membered ring, **7**. In the previous nonhybrid DFT study this step was not investigated, but the barrier was assumed to be very small.[33] However, this assumption could be questioned for that model study, since a

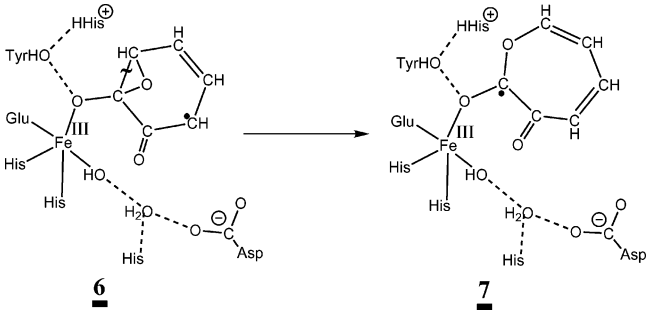

Figure 19. C−C bond cleavage step in the suggested mechanism for extradiol dioxygenase.

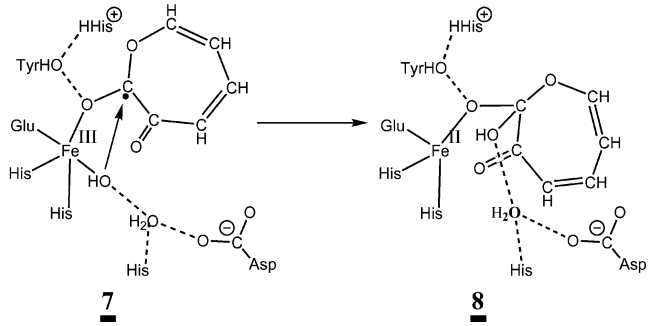

Figure 20. Hydroxyl attack on the substrate in the suggested mechanism for extradiol dioxygenase.

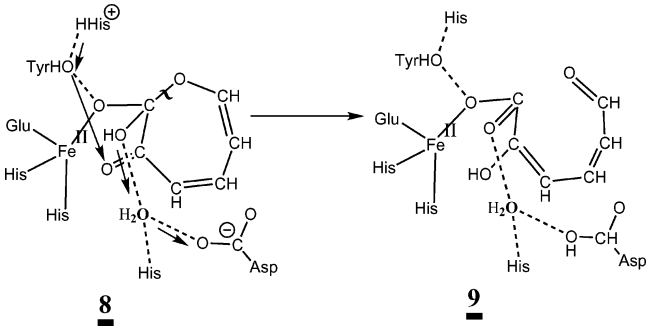

Figure 21. Opening of the seven-membered ring in the suggested mechanism for extradiol dioxygenase.

nonradical epoxide was obtained using that DFT functional. It is concluded from the present results (see also the simple model results discussed above in the beginning of this section) that a radical epoxide could be essential for this step and possibly also for the selectivity.

The minimum for structure **7** is very shallow. The hydroxyl group on Fe(III) can attack the substrate essentially without a barrier, as shown in Figure 20, still keeping the seven-membered ring. There are actually two possibilities for the hydroxyl attack, either on the carbon, as shown in the figure, or on the next carbon in the ring. Both occur with only small barriers, but the former attack is the preferred one and is driven by a larger exothermicity by 7 kcal/mol. This leads to an additional energy lowering of 24.9 kcal/mol on going to structure **8**. A notable feature of this structure is a quite long C−O distance of 1.66 Å, which shows that the ring can rather easily open up.

The final step of the formation of the 2-hydroxymuconaldehyde acid product is the opening of the seven-membered ring (see Figure 21). As indicated by the long C−O distance, this opening occurs with only a negligible barrier, leading first to a dianionic substrate. A proton on the substrate is lost to Asp244

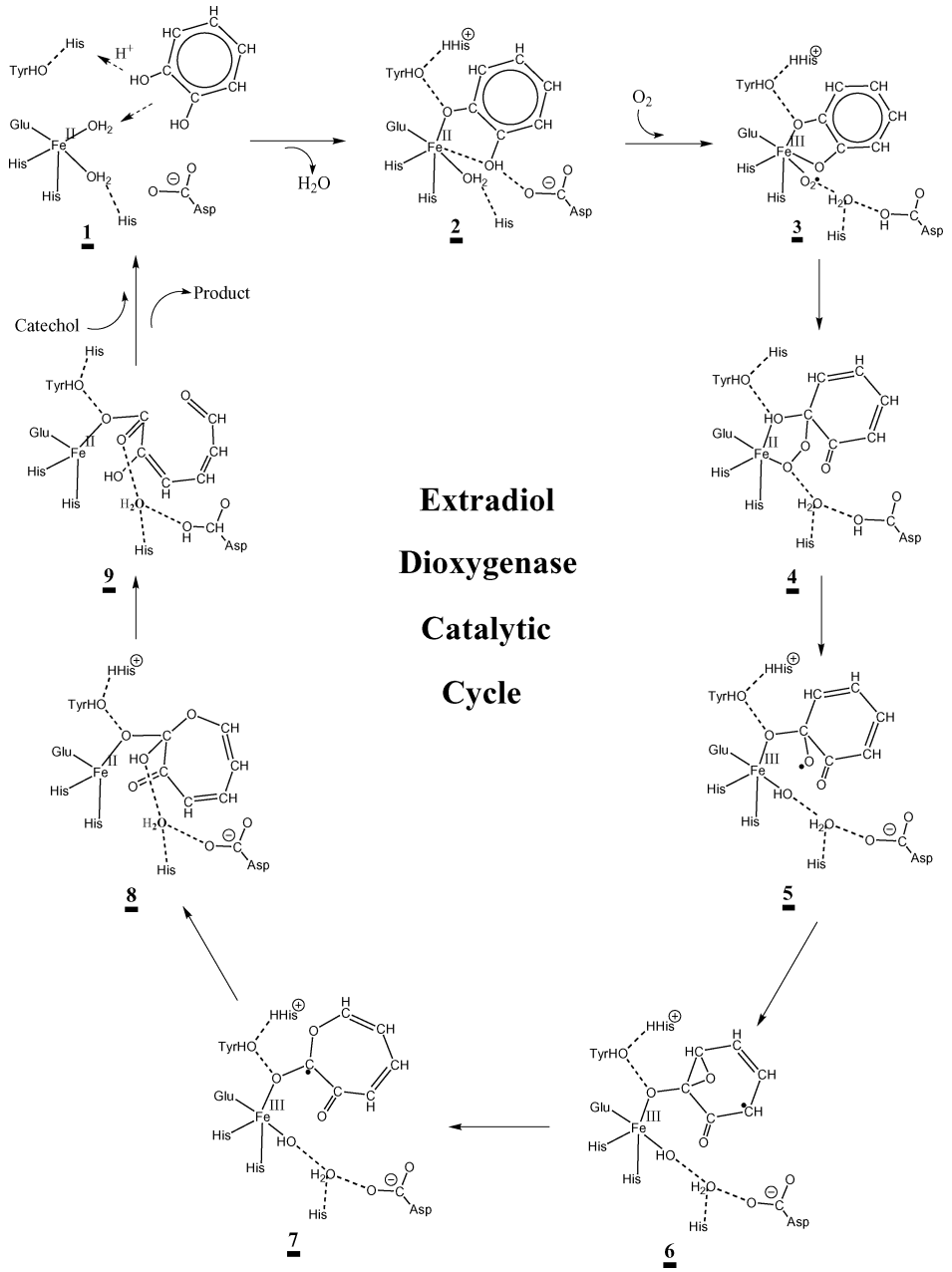

Figure 22. Suggested catalytic cycle for extradiol dioxygenase.

in the ring-opening process. The dianionic substrate is first oriented with its oxygens trans to Glu260 and His210. The exothermicity of this part is 17.4 kcal/mol. Later on, a reorientation occurs so that the oxygens of the dianionic substrate now are trans to His210 and His 146, instead. This leads to an additional energy lowering of 4.9 kcal/mol. From this point, the proton on His241 can now move over to the substrate to form a monoanion. This step is only slightly uphill by 2.6 kcal/mol, forming structure **9**. It should be noted that the substrate of this structure is schematically drawn in Figure 21 to show the changes of the bonding patterns rather than the correct structure, where the atoms would hide each other. The step where the neutral substrate is finally formed was only briefly studied. A straightforward calculation of this part indicates that this step is endothermic but should be driven either by a large entropy gain or by a binding of the next substrate and water.

IV. Conclusions

The presently suggested catalytic cycle for extradiol dioxygenase is summarized in Figure 22, and the energetics for the first part of the cycle is shown in Figure 23. The cycle starts with the binding of catechol. The full energetics for this step has not been studied here, and the energy for this step is therefore not given. Since the structure with bound catechol has been observed experimentally, the binding has to be exergonic. When catechol binds, it loses a proton to become anionic. The most favorable position for the proton was found to be His241. The next step involves the binding of dioxygen. In this process, the water molecule originally bound to iron is moved out to the second shell. It should be noted that entropy effects are not included in the energies, since these cannot accurately be obtained when some atoms are frozen from the X-ray structure. The only step where these effects are likely to be important is

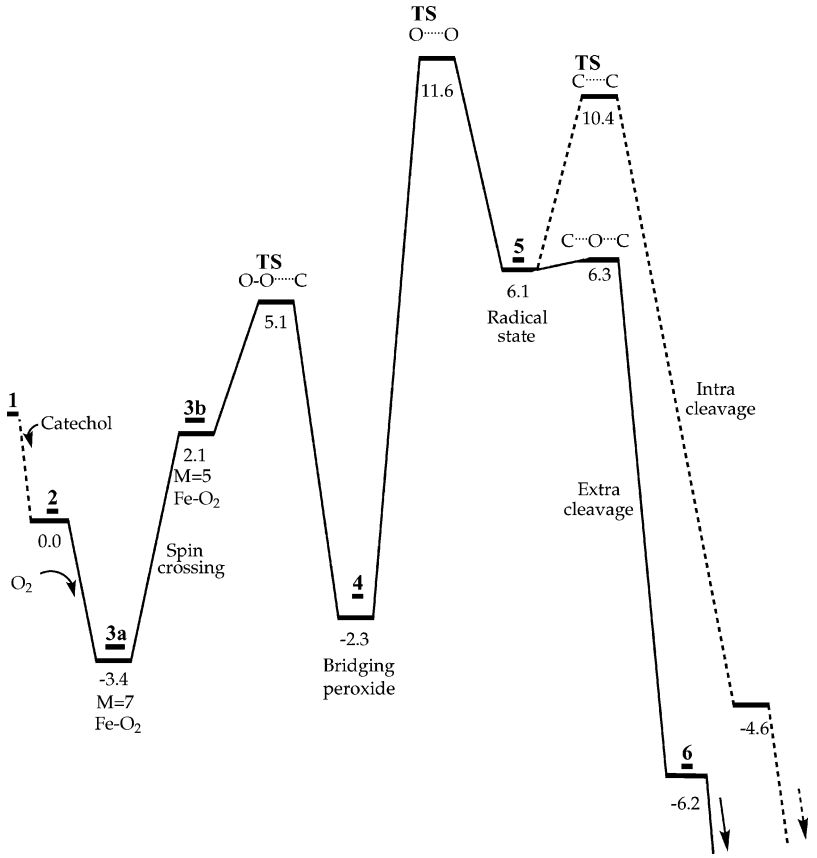

Figure 23. Energetics for the first part of the suggested catalytic cycle of extradiol dioxygenase. The numbers for the structures are those from Figure 21.

where dioxygen binds to iron. The loss of entropy in binding dioxygen will be partly compensated by a gain of entropy as water is released from iron. Still, the binding of dioxygen is expected to be endergonic by up to 5 kcal/mol. With an endergonic binding of dioxygen, a direct experimental observation of this structure is unlikely. It is interesting, in this context, to note that only one structure of a non-heme iron enzyme with bound dioxygen has been observed, and this is for naphthalene dioxygenase.[62] However, the reason this species could be observed in that case is most likely that (at least) one electron is simultaneously transferred to the non-heme iron complex from a diiron Rieske cluster in another part of the enzyme.[58] The situation is thus quite different from the one in extradiol dioxygenase.

The next step of the catalytic cycle involves a spin-crossing from the initial septet (**3a**) to a quintet surface (**3b**), 5.5 kcal/mol higher in energy. On this quintet surface, both dioxygen and the catechol are radicals but with opposite spin. This situation is thus well set up to form a bridging peroxide bond between iron and catechol. This bond formation goes over a barrier 8.5 kcal/mol higher than the septet reactant (**3a**). The product (**4**) is 1.1 kcal/mol higher than the reactant and is therefore also unlikely to be observed by experiments. So far, this mechanism is in agreement with most mechanisms suggested experimentally for the extradiol dioxygenases.[3,4,18,27,34]

After the peroxide formation, the O−O bond is cleaved, and this is suggested to be the rate-limiting step. The barrier is 15.0 kcal/mol with respect to the septet reactant. It can be noted that, even if 7−8 kcal/mol is added for the entropy loss when dioxygen binds to iron, the barrier would still be below 20 kcal/mol (counted from the new resting state **2**). The cleavage of the O−O bond is mainly homolytic. However, the product has partly radical and partly anionic character, which is one of the most important results of the present study and decides the extradiol selectivity. The product **6** is at an energy of 6.1 kcal/mol, making the O−O bond cleavage itself endothermic by 8.4 kcal/mol.

The selectivity of the enzyme is decided in the next step. The barrier for extradiol cleavage is essentially zero, while the one for intradiol cleavage is 4.3 kcal/mol. This would lead to a computed extradiol selectivity of about 1000:1, but this is a very uncertain number. The origin of the selectivity has been analyzed and found to be due to the partly anionic character of the intermediate formed after O−O bond cleavage. This was best seen when the positive charge on His241 was removed, which led to a more radical intermediate and to a preference for intradiol cleavage instead. The high sensitivity of the selectivity is in line with results from mutation studies[38] and biomimetic studies.[3,39]

In the presently suggested mechanism, the O−O bond is cleaved before the C−C bond. However, since there is essentially no barrier for the extradiol C−C bond cleavage itself, the mechanism can instead be termed concerted but nonsynchronous, in analogy to a similar two-step mechanism for the P450 enzymes. The conclusion drawn from several types of models is that no TS where the O−O and C−C bonds are

(62) Karlsson, A.; Parales, J. V.; Parales, R. E.; Gibson, D. T.; Eklund, H.; Ramaswamy, S. *Science* **2003**, *299*, 1039−1042.

cleaved simultaneously exists for the present methods and models, and therefore no direct comparison can be made to the TS in Figure 13. The suggested mechanism is also different from the one suggested previously on the basis of DFT calculations,[33] since a major component of the present mechanism is of radical type. On the other hand, the occurrence of the O−O cleavage prior to the C−C cleavage and the essential role of a protonation of one of the oxygens of dioxygen are quite similar for the two theoretically deduced mechanisms.

JA0493805